Available online at www.sciencedirect.com
SCIENCE DIRECT®
Cement & Concrete Composites 27 (2005) 93–101
Cement & Concrete Composites
www.elsevier.com/locate/cemconcomp

Analytical simulation of pull-out tests—the direct problem

B. Banholzer [a,*], W. Brameshuber [a], W. Jung [b]

[a] *Institute of Building Materials Research, Technical University of Aachen (ibac), Schinkelstraße 3, 52062 Aachen, Germany*
[b] *Institute for Pure and Applied Mathematics, Technical University of Aachen, 52062 Aachen, Germany*

Received 2 April 2003; accepted 5 January 2004

Abstract

In recent years many researchers developed analytical expressions to predict the bond stress versus slip response and the bond stress distribution for different types of pull-out tests, shear tests, etc. However, the models are mainly based on only a limited number of free parameters which can be fitted and therefore a general mathematical description of the bond law is restricted. In this study an analytical model is derived which allows the calculation of a load displacement distribution of a pull-out test on basis of a general mathematical description on the bond stress versus slip relation, assuming a N-piecewise linear bond law with no limitation of N. A short introductory example is given, which clarifies the proposed solution routine and it is shown that a simulation based on the proposed model fits the experimental results of pull-out tests very well.

Keywords: Pull-out test; Analytical model; Bond stress versus slip relationship

1. Introduction

Even in modern materials research there is currently no straightforward experimental method to determine the bond stress versus slip relationship of a fiber/matrix system and the corresponding stress distribution at the interface. Nevertheless, there is growing recognition among researchers that these interfacial properties of a composite are of primary importance for an understanding of the composite's overall behavior and performance. Therefore many researchers have developed analytical and numerical models to yield the bond stress versus slip response and the bond stress distribution on basis of experimental results of different types of single and multifiber pull-out tests, single fiber fragment tests, mircodebond tests and fiber push-in tests.

In general it may be distinguished between two different kinds of analytical models based on force equilibrium considerations and relating to an axisymmetric idealization of the pull-out problem: (I) the perfect interface model and (II) the cohesive interface model. Whereas the perfect interface model, also known as "shear-lag" model is mainly used for analysis of stress transfer problems in resin matrix composites (for example, carbon/epoxy), the cohesive (imperfect interface) model is frequently applied to analyze cement based matrix composites (for example steel fiber/concrete). The principle difference between these two approaches is that in the first case a "perfect interface" is assumed, i.e. no slip between fiber and matrix is allowed and displacements and tractions are continuous at the interface. This displacement continuity requirement is abandoned when the interface is assumed to be imperfect in case of the cohesive interface model. To understand this imperfection let us imagine a thin transition zone of thickness ζ between the constituents (with $\zeta \ll d$ being the diameter of the fiber), called by many authors the interphase, which has properties different from fiber and matrix. For e.g. a steel fiber/cement based matrix system such an interphase was observed by [1], consisting of a calcium hydroxide layer, and a porous layer of calcium silicate hydrates and ettringite. If the stiffness of this transition zone is much smaller than that of the adjoining constituents, the deformation in this zone may be of equal or greater order than the deformations of the stiffer fiber u_F and matrix u_M respectively. This interphase deformation can be expressed by the deformation difference between the adjoining fiber and matrix, the slip $s = u_F - u_M$. If now this real existent interphase is idealized due to its small thickness to become a surface,

* Corresponding author. Fax: +49-241-809-2139.
E-mail address: banholzer@ibac.rwth-aachen.de (B. Banholzer).

0958-9465/$ - see front matter © 2004 Elsevier Ltd. All rights reserved.
doi:10.1016/j.cemconcomp.2004.01.006

Nomenclature

A_F	cross sectional area of the fiber
A_M	load carrying area of the matrix
D	diameter of matrix surrounding the fiber
d	fiber diameter
E_F	modulus of elasticity of fiber in tension
E_M	modulus of elasticity of matrix in compression
F	force in the fiber at a location x
L	embedded length of fiber
m_i	slope of the N-piecewise linear normalized shear flow versus slip relation in an interval i
P	pull-out force
s	slip of the fiber at a location x
s_{cr}	slip at the maximum bond strength τ_{cr}
s_i	slip at the upper-bound of an interval i of the piecewise defined normalized shear flow versus slip relation
s_{i-1}	slip at the lower-bound of an interval i of the piecewise defined normalized shear flow versus slip relation
T	normalized shear flow at a location x
T_i	normalized shear flow corresponding to a slip s_i and a location x_i
T_{i-1}	normalized shear flow corresponding to a slip s_{i-1} and a location x_{i-1}
q	normalized force in the fiber at a location x
q_i	normalized force in the fiber corresponding to a slip s_i and a location x_i
q_{i-1}	normalized force in the fiber corresponding to a slip s_{i-1} and a location x_{i-1}
u_F	absolute displacement of the fiber at a location x
u_M	absolute displacement of the matrix at a location x
x	location in the fiber
ε_F	strain of the fiber at a location x
ε_M	strain of the matrix at a location x
γ	relative compliance
φ	normalized pull-out force
τ	shear stress in the fiber at a location x
τ_{cr}	bond strength of the composite
τ_i	shear stress in the fiber at an interval boundary i
υ	displacement measured at the free fiber end, i.e. $x = 0$
ω	displacement applied at the loaded fiber end, i.e. $x = L$

i.e. an interface, then this displacement difference becomes a displacement discontinuity. The distinctive feature of this idealization lies in the recognition that the shear stress between fiber and matrix τ at any point of the fiber x is a function of the slip s at that fiber segment dx. This function $\tau(s)$ is called the bond stress versus slip relation (BSR) or bond law. Experimental tests carried out by [2,3] on steel fiber/cement based matrix systems confirmed this relation between fiber slip and bond stress in the interphase.

However, until today all proposed analytical models are only capable to calculate a load versus displacement relation $P(\omega)$ of a pull-out test on basis of a given bond law $\tau(s)$ (direct problem, $\tau(s) \rightarrow P(\omega)$). Also most of the studies pertaining to a finite element analysis of the stated problem, e.g. [5] or [6], apply only this direct evaluation method of $P(\omega)$ for a given $\tau(s)$. So far it is not possible to analytically determine a bond stress versus slip relation for a given pull-out curve (inverse problem, $P(\omega) \rightarrow \tau(s)$). Hence, to actually derive such a bond stress versus slip relation for a material combination, bond parameters have to be assumed, a pull-out curve simulated, and compared to the experimental data from a pull-out test. In a fitting or optimization process the best approximation is found and so the bond law is derived. Based on the fact, that even this direct simulation of a pull-out test causes considerable difficulties due to mathematical problems and a simultaneous optimization of many parameters is quite difficult to carry out, these derived bond stress versus slip relations are based only on a limited number of free parameters and hence a general mathematical description of the bond law is restricted. Reviews of such available analytical studies pertaining to bond and pull-out of fibers were conducted at different stages by [7–12] and finally in the state of the art report on "Bond of reinforcement in concrete" [13].

The principal aim of the present study is therefore to derive an analytical model which allows the calculation of a load displacement distribution of a pull-out test on basis of a general mathematical description of the bond stress versus slip relation, assuming a N-piecewise linear bond law with no limitation of N (direct problem, $\tau(s) \rightarrow P(\omega)$). On the basis of such a multilinear bond stress versus slip relation a good description of the reaction of a fiber/matrix system under a pull-out load can be achieved, as will be shown by an example. The presented formulation is also the basis to derive a mathematical method to solve the inverse problem ($P(\omega) \rightarrow \tau(s)$), which will be presented in [4] and will allow the straightforward evaluation of experimental data, i.e. the bond stress versus slip relation $\tau(s)$ can be recovered directly from the observed load displacement curve $P(\omega)$ (inverse problem). Hence no optimization process is needed and so the number of parameters describing the bond law not limited.

2. The direct boundary value problem

The mathematical representation of the pull-out problem based on the stress criterion is generally expressed by two boundary conditions and a second order differential equation derived on basis of two equations of equilibrium, an equation of compatibility and Hooke's law. In almost all of the reviewed studies relating to such a model, among others [14–16], this differential equation is expressed in terms of the forces and stresses in the fiber, respectively, e.g.

$$F_F'' - \lambda^2 F_F = 0 \tag{1}$$

where F_F corresponds to the force in the fiber at a location x and λ is a material parameter which includes the bond stress versus slip relation. This second order differential equation idealizes a cylindrical fiber of diameter d under a pull-out load P and embedded over a length L in an outer cylinder of diameter D representing the matrix of the composite material (Fig. 1). The system is loaded as shown in Fig. 2.

Note that in Eq. (1) and also during the following derivation the axial stresses and strains of both fiber and matrix are taken independent of the radial coordinate because as mentioned before the stiffness of the interphase is assumed to be smaller than that of the adjoining constituents. Thus, lateral strains as well as stresses occurring in the matrix e.g. due to a lateral contraction may be neglected and the axial stresses taken as average axial stresses and hence independent of the radial direction. If it is found in the future that these assumptions do not prove true, a higher order differential equation or a partial differential equation has to be adopted to represent the pull-out problem in a mathematical form which might complicate the following solution procedure.

Another possible approach is to express the pull-out problem with respect to the local slip s, see e.g. [15,17]. After substituting the unit elongation up to the proportional limit of the matrix and the fiber respectively (Hooke's law)

$$\varepsilon_M = \frac{F_M}{A_M E_M}, \quad \varepsilon_F = \frac{F_F}{A_F E_F} \tag{2}$$

into the first derivative of the difference of the local displacements ($s = u_F - u_M$, see Fig. 1), (equation of compatibility),

$$\frac{ds}{dx} = \varepsilon_F - \varepsilon_M \tag{3}$$

differentiating this result again with respect to x and using the general equilibrium of forces in a cross section of fiber and matrix (Fig. 2)

$$F_F + F_M = 0 \tag{4}$$

and the equilibrium of forces on a infinitesimal element of the fiber of length dx (Fig. 2)

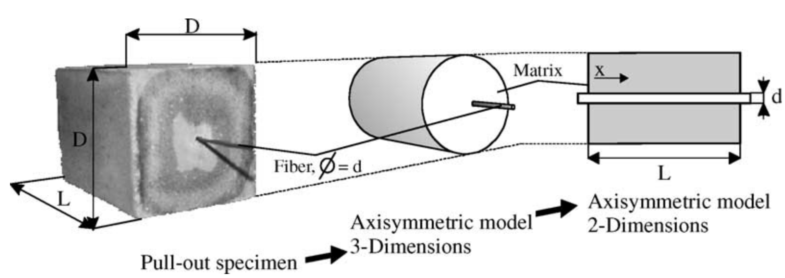

Fig. 1. Original pull-out specimen and axisymmetric models for 3 and 2 dimensions.

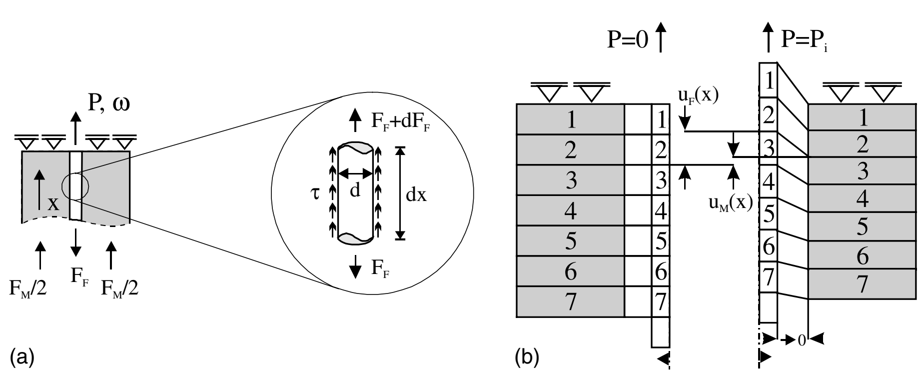

Fig. 2. (a) Global equilibrium of forces and equilibrium of forces on a small element of the fiber. (b) Absolute displacements of the fiber $u_F(x)$ and matrix $u_M(x)$ as result of loading.

$$\frac{dF_F}{dx} = \pi d\tau(s) \tag{5}$$

we obtain the following second order differential equation in terms of the slip s between fiber and matrix

$$s'' = \pi d\left[\frac{1}{A_F E_F} + \frac{1}{A_M E_M}\right]\tau(s) = T(s),$$
$$T(s) = \pi d\gamma\tau(s), \tag{6}$$
$$\gamma = \frac{1}{A_F E_F} + \frac{1}{A_M E_M}$$

where τ corresponds to the interfacial shear stress, F_F to the force in the fiber and F_M to the force in the matrix at a location x. A_F and A_M are the load carrying areas of the fiber and matrix, and E_F and E_M are the moduli of elasticity of the fiber and the matrix respectively. Eq. (6) represents the basic relationship between the second order derivative of the local slip s and the local bond stress τ which is again assumed to be a function of the local slip. To allow a general mathematical description of the bond law a N-piecewise linear relation (N is not limited) between the bond stress τ and the slip s as shown in Fig. 3 is used and normalized for simplicity of the following derivation: $T(s) = \pi d\gamma\tau(s)$. To distinguish between the bond stress versus slip relation $\tau(s)$ and $T(s)$, $T(s)$ is called hereafter the *normalized bond flow versus slip relation*. This function $T(s)$ can be expressed for an interval $i = [s_{i-1}, s_i]$ as

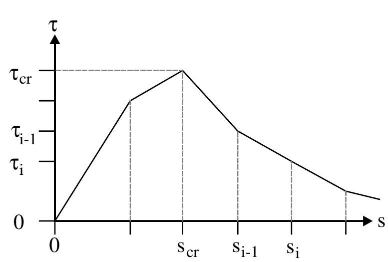

Fig. 3. N-piecewise linear relation between the bond stress τ and the slip s.

$$T(s) = m_i(s - s_{i-1}) + T_{i-1}, \quad m_i = \frac{T_i - T_{i-1}}{s_i - s_{i-1}},$$
$$T_0 = s_0 = 0 \tag{7}$$

Consequently the force F_F in the fiber is normalized as well.

$$q(x) = \gamma F_F(x) = s'(x) \tag{8}$$

From Fig. 2 the boundary conditions can be deduced. The force in the fiber at $x = L$ corresponds to the pull-out load P, hence we have $s'(L) = q(L) = \gamma P = \varphi$. Knowing, that at $x = 0$ the force in the fiber is zero we find $s'(0) = q(0) = 0$. Likewise we can state that the displacement at the loaded end of the fiber yields $s(L) = \omega$. Assuming the slip s at the free fiber end to be υ ($s(0) = \upsilon$) and denoting the coordinate of the fiber by $0 \leqslant x \leqslant L$, the mathematical representation of the pull-out problem can be expressed either as boundary value problem (BVP)

$$s'' = T(s), \quad s'(0) = q(0) = 0, \quad s(L) = \omega \tag{9}$$

or as a corresponding initial value problem (IVP)

$$s'' = T(s), \quad s'(0) = q(0) = 0, \quad s(0) = \upsilon \tag{10}$$

Fig. 4 illustrates the boundary and initial conditions in Eqs. (9) and (10) respectively. This notation has the advantage that the normalized bond law $T(s)$ is explicitly adopted in the second order differential equation and related directly to all the measurands of the pull-out test by the boundary and initial conditions respectively.

The IVP (Eq. (10)) can be solved easily in an iterative process for any given $T(s)$ and υ with a numerical integration procedure, e.g. the RUNGE–KUTTA-Procedure, and the help of a popular math-program (e.g. Maple®). However, to allow a better insight in the processes during a pull-out of a fiber, to give a complete solution routine to simulate a pull-out test, and to work out the basics for the inverse boundary value problem $P(\omega) \to \tau(s)$, the following derivation of a solution procedure is listed.

During a pull-out test a displacement ω is applied at the loaded end of the fiber and continuously increased until the fiber is pulled out of the surrounding matrix.

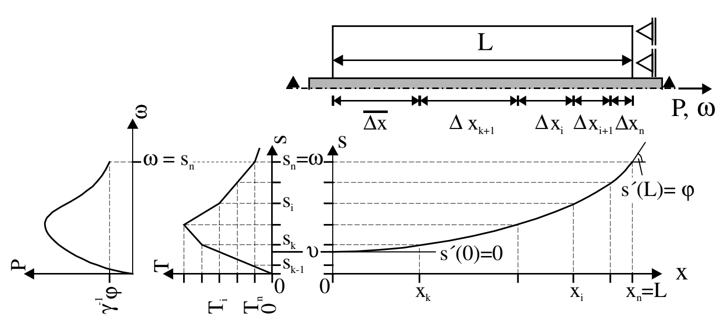

Fig. 4. Slip distribution and boundary conditions at the left and right side of the system.

The corresponding resulting force P is measured and recorded as a function of ω.

In the analytical simulation, similar to the actual pull-out test, the displacement ω is given and the resulting pull-out force $\gamma^{-1} \cdot \varphi$ has to be determined in an iterative procedure, such that the boundary condition at the free fiber end $s'(0) = 0$ is satisfied (compare Fig. 4 and Eq. (9)). For simplification of the following derivation and discussion we consider the situation at a certain time during the pull-out test, where a displacement ω is applied at the loaded end of the fiber and a corresponding pull-out force of $\gamma^{-1}\varphi$ is measured (see Fig. 4, left). This point of time is chosen such, that the introduced displacement ω at $x = L$ during the simulated pull-out test equals the slip of the upper-bound of the interval n of the selected piecewise linear function $T(s)$, i.e. $\omega = s_n = s(L)$. The corresponding normalized pull-out force is $\varphi = q_n = s'(L)$. Fig. 4 (right) shows these two parameters in the slip versus axial coordinate curve. The applied displacement ω corresponds to the slip s_n at the location $x_n = L$ and the normalized pull-out force φ to the slope s'_n at the location $x_n = L$. In a similar way the index i for $i = 0$ to n mentioned in the following derivation associates the slips s_i at the upper-bound of the interval $i = [s_{i-1}, s_i]$ of the piecewise defined normalized shear flow versus slip relation $T(s)$ with the corresponding normalized shear flows $s'' = T_i$ and fiber forces $s' = q_i$ as well as slips $s = s_i$ at a location x_i (see Fig. 4, middle/right). Keeping this in mind we can proceed as follows. Using a reduction of order method

$$\frac{1}{2}(s'^2)' = s''s' = T(s)s'$$

similar to [15], knowing that the lower boundary for s is υ (the slip at $x = 0$, see Fig. 4), and substituting a function $A(s)$ for the integral term of $2T(s)$, $s'' = T(s)$ in Eq. (10) yields

$$s'^2 = 2\int_{\upsilon}^{s} T(\bar{s})\,\mathrm{d}\bar{s} = A(s) - A(\upsilon), \quad A(s) := 2\int_{0}^{s} T(\bar{s})\,\mathrm{d}\bar{s} \tag{11}$$

Eq. (11) states, that the difference of the integral of $T(s)$ in the interval $[0, \upsilon]$ and $[0, s]$ respectively corresponds to the difference of the squared tensile forces in the fiber at $x = 0$ and x. Hence the force in the fiber q_{i-1} at a location x_{i-1} ($s'(x_{i-1}) = q_{i-1}$) can be determined for a given $s'(x_i) = q_i$, if Eq. (11) is evaluated for $s = s_i$ and $s = s_{i-1}$ and the results are subtracted. This yields

$$\begin{aligned} s_i'^2 - s_{i-1}'^2 &= 2\int_{\upsilon}^{s_i} T(\bar{s})\,\mathrm{d}\bar{s} - 2\int_{\upsilon}^{s_{i-1}} T(\bar{s})\,\mathrm{d}\bar{s} \\ &= 2\int_{s_{i-1}}^{s_i} T(\bar{s})\,\mathrm{d}\bar{s} = A(s_i) - A(s_{i-1}) \\ &= m_i(s_i - s_{i-1})^2 + 2T_{i-1}(s_i - s_{i-1}) \end{aligned} \tag{12}$$

Denoting $s'_i = q_i$ and $s'_{i-1} = q_{i-1}$ and rearranging gives

$$q_{i-1}^2 = q_i^2 - m_i(s_i - s_{i-1})^2 - 2T_{i-1}(s_i - s_{i-1}) \tag{13}$$

Eq. (13) states, that for a given force $q_i = s'_i$ in the fiber at a location x_i corresponding to the upper-bound s_i of the interval i of the piecewise linear normalized bond flow versus slip function $T(s)$, a force $q_{i-1} = s'_{i-1}$ in the fiber at a location x_{i-1} may be calculated which corresponds to the lower-bound s_{i-1} of the interval i. See Fig. 4.

As mentioned before, a solution for the BVP in Eq. (9) is found if a pull-out force $\varphi = q_n$ can be determined, such that

- the slope s' and hence the force q at a location $\hat{x}$ in the fiber is zero (condition I),
- and that the location where $s' = 0$ is at $\hat{x} = 0$, i.e. the free fiber end (condition II).

See Fig. 5. For $i = n$ the force q_n is known to be the normalized pull-out force $s'(x = L) = q_n = \varphi$. Because the normalized bond flow versus slip relation is also known, the forces in the fiber can be calculated recursively with the help of Eq. (13), starting from $i = n$.

During this recursive process it will occur, that a $q_{k-1}^2 < 0$ is calculated according to Eq. (13) but q_k^2 is still greater zero. This states, that the slope of the function $s(x)$ has changed its sign between the locations x_{k-1} and x_k, see Fig. 5. Hence the condition $s' = q = 0$ is satisfied in the range $x_{k-1} < \hat{x} < x_k$. Because the locations x_{k-1} and x_k also correspond to the lower-bound s_{k-1} and upper-bound s_k respectively of the interval k of the normalized bond flow versus slip relation (Fig. 4) we further know, that the slip of the free fiber end υ is in the range of $s_{k-1} \leqslant \upsilon < s_k$ (Fig. 5). Thus it can be stated, that s' turns zero somewhere in the interval k.

However, this recursive determination of the fiber forces using Eq. (13) only guarantees that the slope is zero at a $\hat{x}$ (condition I) but not, that $s' = 0$ at the location $\hat{x} = 0$ (condition II) because $\hat{x}$ depends on the chosen φ.

To determine the location $\hat{x}$ where $s' = 0$, the sum of the incremental lengths $\Delta x_i = x_i - x_{i-1}$ has to be determined (compare Fig. 5). Only if this sum yields the

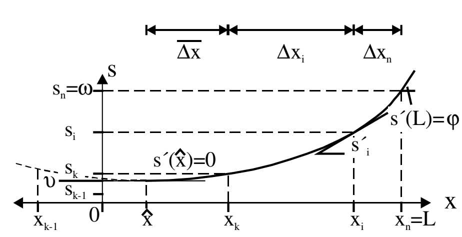

Fig. 5. Slip distribution with a zero slope in the interval k at $\hat{x}$ (condition I).

embedded length L, the above mentioned condition II that $s' = 0$ at $\hat{x} = 0$ is satisfied.

The summation of the incremental lengths Δx_i can be written as follows (compare Fig. 5)

$$L = \overline{\Delta x} + \sum_{i=k+1}^{n} \Delta x_i \tag{14}$$

with k being the interval number evaluated before, where s' turns zero.

Δx_i and $\overline{\Delta x}$ of Eq. (14) can be determined as follows. Evaluating Eq. (11) for s and $s = s_{i-1}$, subtracting the results, and rearranging yields (similar to Eq. (12))

$$s' = \frac{\mathrm{d}s}{\mathrm{d}x} = \sqrt{m_i(s - s_{i-1})^2 + 2T_{i-1}(s - s_{i-1}) + s'^2_{i-1}} \tag{15}$$

After a separation of variables, substituting $q_{i-1} = s'_{i-1}$ and integrating we get for the lower-bound s_{i-1} and upper-bound s_i of the interval i of the $T(s)$ function

$$\Delta x_i = \int_{s_{i-1}}^{s_i} \frac{\mathrm{d}\hat{s}}{\sqrt{m_i(s - s_{i-1})^2 + 2T_{i-1}(s - s_{i-1}) + q^2_{i-1}}} \tag{16}$$

Eq. (16) can be evaluated as follows. For $m_i > 0$ we obtain

$$\Delta x_i = \frac{1}{\sqrt{m_i}} \ln\left[\frac{\sqrt{m_i} q_i + T_i}{\sqrt{m_i} q_{i-1} + T_{i-1}}\right] \tag{17}$$

and for $m_i < 0$

$$\Delta x_i = \frac{1}{\sqrt{-m_i}} \arcsin\left[\frac{\sqrt{-m_i}(T_i q_{i-1} - T_{i-1} q_i)}{T^2_{i-1} - m_i q^2_{i-1}}\right] \tag{18}$$

The last incremental length $\overline{\Delta x}$ can be determined knowing that the force in the fiber at $\hat{x}$ is zero ($q^2_{k-1} \equiv 0$). Substituting

$$s_k - s_{k-1} = \frac{T_k - T_{k-1}}{m_k}$$

according to Eq. (7), and $q^2_{k-1} \equiv 0$ in Eq. (13) yields after a few transformations for the interval k

$$\overline{T}^2 = T_k^2 - m_k q_k^2 \tag{19}$$

where $T_{k-1} \equiv \overline{T}$ is the shear stress at $\hat{x}$. Using $q^2_{k-1} \equiv 0$, $T_{k-1} \equiv \overline{T}$, and Eq. (19) in either Eq. (17) or Eq. (18) gives $\overline{\Delta x}$ for $m_k > 0$ and $m_k < 0$ respectively. This yields e.g. for $m_k > 0$

$$\overline{\Delta x} = \frac{1}{\sqrt{m_k}} \ln\left[\frac{\sqrt{m_k} q_k + T_k}{\sqrt{T_k^2 - m_k q_k^2}}\right], \quad m_k > 0 \tag{20}$$

The above listed procedure can be summarized as follows:

A $\varphi = q_n$ has to be found in an iterative procedure for a given displacement $s(x_n = L) = \omega$ such that the incremental lengths Δx_i (for $m_i > 0$ according to Eq. (17) and for $m_i < 0$ according to Eq. (18)) sum up to the embedded length L according to Eq. (14). The lower-bound k in Eq. (14) is evaluated by using Eq. (13) in a recursive way starting from $i = n$ until a $(q_{k-1})^2 < 0$ is determined and hence the interval number k is found in which the force in the fiber turns zero.

If a $\varphi = q_n$ is found satisfying the boundary condition $s'(0) = 0$ the solution to the BVP listed in Eq. (9) is found and hence the resulting force $P = \gamma^{-1}\varphi$ for an applied displacement ω at the loaded end of the fiber is determined. To derive a complete load displacement diagram for a given normalized shear flow relation $T(s)$ and hence a given shear stress relation $\tau(s)$, initial conditions $P = \gamma^{-1}\varphi$ have to be found for many load steps of a pull-out test such that Eq. (14) is always satisfied. Nevertheless, with the help of a computer routine where the above described numerical iteration process is included, the right initial conditions φ can be found quite easily, and hence a complete pull-out test is simulated.

3. Example

To clarify this procedure a short introductory example is given based on the bond stress versus slip relation and the experimental results presented in the state of the art report on "Bond of reinforcement in concrete" [13, pp. 57/58]. Although a reinforcement bar offers a different surface geometry in comparison to an ordinary steel fiber and the resulting pull-out process is accompanied by transverse microcracking, local crushing of the porous layer around the rib and eventually by a splitting of the surrounding concrete, the pull-out response of small diameter steel bars is according to [13] mainly depending on the mechanical properties in a close by microzone, similar to the interphase in a steel fiber/matrix system. As the numerical predictions of the pull-out response presented in [13] show a high discrepancy compared to the experimental test results, this example is also taken to illustrate the advantages of the proposed solution routine.

The chosen system consists of an ordinary steel reinforcement bar with a Young's modulus of $E_F = 210$ kN/mm^2 and diameter of $d = 16$ mm and a normal-strength concrete with a Young's modulus of $E_M = 354$ kN/mm^2 and a load carrying area of $A_M = 10,000$ mm^2 (estimated). Until today the effective load carrying area of a matrix during a pull-out test has not been determined explicitly. The embedded length L is taken to be 40 mm (2.5 times the bar diameter). The bond stress versus slip relation given in [13, pp. 57/58] is shown in Table 1 using a γ according to Eq. (6) of $\gamma = 2.40 \times 10^{-8}$ kN^{-1}.

Starting at a given displacement $\omega = 0$, the begin of the pull-out test, we know that the corresponding pull-out load equals $\varphi = P = 0$.

For the next load step $n = 1$ the given introduced displacement at the loaded fiber end is $\omega = 0.25$ mm. Using Eq. (20) $\varphi = q_1$ can be calculated straight forwardly to be 3.42×10^{-4} because for $n = 1$ $\overline{\Delta x}$ is known

Table 1
Bond stress versus slip relation according to [13, pp. 57/58]

i	Slip s_i/mm	Shear stress τ_i/(N/mm^2)	Generalize shear flow T_i/(1/mm)	Gradient m_i/(1/mm^2)
0	0.00	0.00	0.00	
1	0.25	7.24	8.72E−06	3.49E−05
2	0.50	9.55	1.15E−05	1.11E−05
3	0.75	11.23	1.35E−05	8.10E−05
4	1.00	12.60	1.52E−05	6.60E−05
5	3.00	12.60	1.52E−05	0.00
6	4.00	5.04	6.07E−06	−6.07E−06
7	12.0	0.00	0.00	−3.68E−07

to be L, $k = 1$, and hence the summation term in Eq. (14) can be neglected. m_1 is known to be greater zero (Table 1). Thus P is 14.28 kN.

To determine φ for $n > 1$ Eqs. (13) and (14) respectively are used. Because all of the gradients m_i for $i = 1$ to 2 are positive for the given example (compare Table 1) Eq. (14) can be written as follows for the next load step $n = 2$.

$$L = \overline{\Delta x} + \sum_{i=k+1}^{n=2} \Delta x_i = \frac{1}{\sqrt{m_k}} \ln\left[\frac{\sqrt{m_k} q_k + T_k}{\sqrt{T_k^2 - m_k q_k^2}}\right] + \sum_{i=k+1}^{n=2} \frac{1}{\sqrt{m_i}} \ln\left[\frac{\sqrt{m_i}\varphi_i + T_i}{\sqrt{m_i}\varphi_{i-1} + T_{i-1}}\right] \quad (21)$$

An estimation is made for φ. In the given example $\varphi = q_{n=2}$ is chosen to be 4.57×10^{-4} yielding according to Eq. (13) to a new $q_1^2 = -4.85 \times 10^{-6}$ which is less than zero. This states, that the slip at the free fiber end is no longer in the range of $0 \leqslant \upsilon \leqslant s_1$ but already slipped through to an extend greater than s_1 and therefore the interval in which q turns zero is identified to be $k = 2$. Hence, Eq. (21) yields

$$L = \frac{1}{\sqrt{m_2}} \ln\left[\frac{\sqrt{m_2} q_2 + T_2}{\sqrt{T_2^2 - m_2 q_2^2}}\right] = \frac{1}{\sqrt{1.11\times10^{-5}}} \times \ln\left[\frac{\sqrt{1.11\times10^{-5}}4.57\times10^{-4} + 1.15\times10^{-5}}{\sqrt{(1.15\times10^{-5})^2 - 1.11\times10^{-5}\times(4.57\times10^{-4})^2}}\right] \text{mm} \approx 40 \text{ mm}$$

Because all initial conditions are kept, a φ of 4.57×10^{-4} is determined for this load step, corresponding to a pull-out force P of 19.04 kN.

Writing a numerical procedure and following the above listed flow of the algorithm the resulting load versus displacement diagram for the given example can easily be calculated (Fig. 6). Comparing the analytical results based on the bond law proposed by [13] with the experimental outcomes a discrepancy is found (Fig. 6).

Using now a modified multilinear shear stress versus slip relation (Table 2) and the introduced analytical model, the discrepancy between the experimental test results and the numerically calculated load versus displacement relationship is reduced (Fig. 6). This states, that by using the presented model which is based on such a multilinear bond stress versus slip relation a good description of the reaction of a fiber matrix system under a pull-out load can be achieved. However, a pull-out test can only be simulated if the underlying bond law is known and therefore the presented and fitted load displacement curve in Fig. 6 could only be obtained, if the bond stress versus slip relation was adapted manually and the resulting load versus displacement relationship compared visually. Therefore it would be quite useful to have a numerical procedure which would allow an automatic determination of a bond stress versus slip relation to a corresponding experimentally found load displacement distribution. This approach is called an inverse boundary value problem.

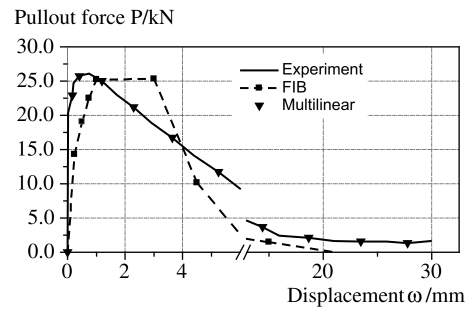

Fig. 6. Pull-out relations: (I) experiment, (II) based on [13, pp. 57/58] and (III) simulation based on a multilinear bond law (Table 1). Note that (III) is congruent with (I).

4. The inverse boundary value problem

As it is found, that there is a straightforward relation between the normalized shear flow $T(s)$ and the corresponding normalized pull-out force $\varphi(\omega)$ it must not only be possible to derive a load versus displacement relation from a given bond stress versus slip relation as it has been shown before but also to derive a bond stress versus slip relation from a given load versus displacement relation. This procedure is based on an inverse boundary value problem. Based on this mathematical

Table 2
Multilinear bond stress versus slip relation

i	Slip s_i/mm	Shear stress τ_i/(N/mm^2)	Generalize shear flow T_i/(1/mm)	Gradient m_i/(1/mm^2)
0	0	0.00	0	
1	0.01	10.14	1.22E−05	0.00122162
2	0.16	11.43	1.38E−05	1.039E−05
3	0.20	12.29	1.48E−05	2.5925E−05
4	0.42	12.82	1.54E−05	2.8883E−06
5	0.75	12.97	1.56E−05	5.2611E−07
6	1.20	12.44	1.50E−05	−1.411E−06
7	1.72	11.43	1.38E−05	−2.3286E−06
8	2.29	10.52	1.27E−05	−1.9256E−06
9	2.91	9.42	1.14E−05	−2.1357E−06
10	3.65	8.32	1.00E−05	−1.791E−06
11	4.39	7.03	8.47E−06	−2.1052E−06
12	5.25	5.84	7.03E−06	−1.6728E−06
13	6.88	4.40	5.30E−06	−1.0592E−06
14	8.50	3.59	4.32E−06	−6.0688E−07
15	10.29	3.06	3.69E−06	−3.5472E−07
16	12.18	2.39	2.88E−06	−4.2518E−07
17	14.42	1.82	2.18E−06	−3.1041E−07
18	15.98	1.19	1.43E−06	−4.8031E−07
19	18.70	1.05	1.27E−06	−6.1704E−08
20	20.98	0.81	9.77E−07	−1.2882E−07
21	23.49	0.77	9.23E−07	−2.1495E−08

principle a numerical procedure can be developed which will allow the inverse determination of the bond stress versus slip relation from a given load versus displacement relationship. In [4] this problem will be discussed in detail.

5. Summary and conclusions

In the present paper an analytical approach is introduced to simulate the pull-out response of a fiber/matrix system in which an N-piecewise linear bond stress versus slip relation is adopted and the number N of the linear intervals assumed is not limited. Hence, if N is taken large, any possible bond law distribution can be approximated, i.e. a general mathematical description of this relation is allowed. In recent studies the bond stress versus slip relation has been applied only with three or four linear sections. Thus the proposed model may be seen as an extensive improvement which guarantees an unrestricted formulation of $\tau(s)$, i.e. a better simulation of the processes occurring during a pull-out. Because it is not possible to find a closed form analytical solution for this approach, a simple numerical solution procedure is presented. Using the experimental results as well as the bond stress versus slip relation presented in the state of the art report on "Bond of reinforcement in concrete" [13, pp. 57/58] and a fitted multilinear bond stress versus slip relation, a short introductory example is given which should clarify the proposed solution routine. Based on this example it is further shown, that the simulated pull-out curve based on the multilinear bond law and calculated with the proposed analytical model fits the experimental results considerably better than the simulation based on the bond stress versus slip relation presented in the state of the art report. This demonstrates, that the analytical solutions to the fiber pull-out problem presented in recent studies and based on a linear or nonlinear elastic pre-debonding behavior, a linear softening branch and a constant and uniform post-elastic frictional bond strength cannot cope with some of the nonlinear abrasion effects observed in the experiments. The proposed cohesive interface model, however, is capable to reflect these processes in the simulation. Although the main assumption of the model, that the pull-out response is predominated by an interphase deformation which is expressed by the deformation difference between the adjoining fiber and matrix, has been verified by experimental tests [2,3] an additional verification of the proposed model on basis of steel fiber pull-out tests with different fiber radii and embedded lengths will be presented in [4] building on the presented work. It will be further shown that the underlying bond stress versus slip relation $\tau(s)$ is a material parameter and hence not dependent on geometric factors of fiber and matrix, e.g. fiber diameter and embedded length.

Based on the proposed derivation the derived solution can furthermore be modified not only to calculate a load versus displacement diagram on the basis of a given shear stress versus slip relation but to actually derive a bond law from experimental results [4]. Certainly this is also possible with an inverse calculation by means of the finite element method. However, the presented numerical solution routine provides a simple and straightforward method to determine the prevailing bond law and avoids time consuming and sometimes nonconvergent optimization procedures.

Thus it will be possible to compare different combinations of materials not only on the basis of particular parameters regarding their bonding characteristics, but rather on the basis of the complete bond law. Furthermore the proposed evaluation method provides the possibility to utilize the identified bond law in more complex numerical studies for the clarification of the load carrying characteristics of fiber reinforced concrete systems. Another important aspect is the characterization of different material combinations regarding the bond qualities. Therefore the presented evaluation method seems to be an appropriate tool to analyze pull-out tests of fibers embedded in a matrix.

Acknowledgements

This project is part of the Collaborative Research Center 532 "Textile reinforced concrete—Basics for the development of a new technoloxgy" and sponsored by the Deutsche Forschungsgemeinschaft (DFG). The support is gratefully acknowledged.

References

[1] Bentur A, Gray RJ, Mindess S. Cracking and pull-out processes in fibre reinforced cementitious materials. In: Third International Symposium on Developments in Fibre Reinforced Cement and Concrete: Rilem Symposium FRC 86, University of Sheffield, England 13–17 July 1986, vol. 2, Vortrag 6.2. Rochdale: RILEM Technical Committee 49-TFR.

[2] Potrzebowski J. Behaviour of the fibre/matrix interface in SFRC during loading. In: Brittle matrix composites, 1. London: Elsevier Applied Science; 1986. p. 455–69.

[3] Potrzebowski J. Debonding processes between steel fibre and cement matrix. In: Brittle matrix composites, 2. London: Elsevier Applied Science; 1986. p. 352–61.

[4] Banholzer B, Brameshuber W, Jung W. Analytical simulation of a pull-out test on basis of an N-piecewise linear bond law—the inverse problem. Cem Concr Compos, in preparation.

[5] Desir J-M, Romdhane MRB, Ulm F-J, Fairbairn EMR. Steel–corrosion interface: revisiting constitutive and numerical modeling. Comput Struct 1999;71:489–503.

[6] Kwak H-G, Kim S-P. Bond–slip behavior under monotonic uniaxial loads. Eng Struct 2001;23:298–309.

[7] Bartos P. Review paper: bond in fibre reinforced cements and concretes. Int J Cem Compos 1981;3:159–77.

[8] Gray RJ. Analysis of the effect of embedded fibre length on fibre debonding and pull-out from an elastic matrix. J Mater Sci 1984; 19(3):861–70.

[9] Nammur G, Naaman AE. Bond stress model for fiber reinforced concrete based on bond stress–slip relationship. ACI Mater J 1989;86(1):45–57.

[10] Shah SP, Ouyang C. Mechanical behavior of fiber-reinforced cement-based composites. J Am Ceram Soc 1991;74(11):2727–38.

[11] Kim J-K, Baillie C, Mai YW, Zhou L-M. Interfacial debonding and fibre pull-out stresses. Part I. Critical comparison of existing theories with experiments. Part II. A new model based on the fracture mechanics approach. J Mater Sci 1992;27:3143–66.

[12] Kim J-K, Mai Y-W. Engineered interfaces in fiber reinforced composites. Amsterdam: Elsevier; 1998.

[13] Federation internationale du beton; fib; FIP; CEB; fib Bulletin No. 10: bond of reinforcement in concrete. State-of-art report. In: fib Bulletin (2000) No. 10. Fédération du Béton, Lausanne, CH, 2000.

[14] Naaman AE, Namur GG, Alwan JM, Najm HS. Fiber pull-out and bond slip. I. Analytical study. II. Experimental validation. Struct Eng 1991;117(9):2769–800.

[15] Bazant ZP, Desmorat R. Size effect in fiber or bar pull-out with interface softening slip. J Eng Mech 1994;120(9):1945–63.

[16] Akatsu T, Tanabe Y, Yasuda E. Crack-bridging processes and fracture resistance of a discontinuous fiber-reinforced brittle matrix composite. J Mater Res 1999;14(4):1316–24.

[17] Somayaji S, Shah SP. Bond stress versus slip relationship and cracking response. ACI Journal 1981 (May–June).